SLAC–PUB–8225
August 1999

Time Dependent $B_s^0 - \overline{B_s^0}$ Mixing Using Inclusive and Semileptonic B Decays at SLD*

The SLD Collaboration**
Stanford Linear Accelerator Center,
Stanford University, Stanford, CA 94309

Abstract

We set a preliminary 95% C.L. exclusion on the oscillation frequency of $B_s^0 - \overline{B_s^0}$ mixing using a sample of 350,000 hadronic Z^0 decays collected by the SLD experiment at the SLC during the 1997-98 run. The analyses determine the b-hadron flavor at production by exploiting the large forward-backward asymmetry of polarized $Z^0 \to b\overline{b}$ decays as well as information from the hemisphere opposite that of the reconstructed B decay. In one analysis, B decay vertices are reconstructed inclusively with a new topological technique, and separation between B_s^0 and $\overline{B_s^0}$ decays exploits the $B_s^0 \to D_s^-$ cascade charge structure. In the other analysis, semileptonic decays are selected and the B decay point is reconstructed by intersecting a lepton track with the trajectory of a topologically reconstructed D meson. The two analyses are combined with a third analysis described elsewhere to exclude the following values of the $B_s^0 - \overline{B_s^0}$ mixing oscillation frequency: $\Delta m_s < 5.2$ ps^{-1} and $11.3 < \Delta m_s < 14.2$ ps^{-1} at the 95% confidence level.

Paper Contributed to the XIX International Symposium on Lepton and Photon Interactions at High Energies, August 9-14, 1999, Stanford, USA.

*Work supported in part by the Department of Energy contract DE–AC03–76SF00515.

1 Introduction

Transitions between B^0 and $\overline{B^0}$ mesons take place via second order weak interactions. In the Standard Model, a measurement of the oscillation frequency Δm_d for B^0_d–$\overline{B^0_d}$ mixing determines, in principle, the value of the Cabibbo-Kobayashi-Maskawa matrix element $|V_{td}|$, which is parameterized in terms of the Wolfenstein parameters ρ and (the CP-violating phase) η, both of which are currently poorly constrained. However, theoretical uncertainties in calculating hadronic matrix elements are large ($\sim 25\%$ [1]) and thus limit the current usefulness of precise Δm_d measurements. Some of these uncertainties cancel when one considers the ratio between Δm_d and Δm_s, leading to a reduced theoretical uncertainty ($\sim$ 5–10%). Thus, combining measurements of the oscillation frequency of both B^0_d–$\overline{B^0_d}$ and B^0_s–$\overline{B^0_s}$ mixing translates into a measurement of the ratio $|V_{td}|/|V_{ts}|$ and provides a stronger constraint on the parameters ρ and η.

Experimentally, a measurement of the time dependence of B^0–$\overline{B^0}$ mixing requires three ingredients: (i) the B decay proper time has to be reconstructed, (ii) the B flavor at production (initial state $t = 0$) needs to be determined, as well as (iii) the B flavor at decay (final state $t = t_{\rm decay}$). At SLD, the time dependence of B^0_s–$\overline{B^0_s}$ mixing has been studied using three different methods, two of which are described below. The third method ("lepton+tracks") is described elsewhere (see Ref. [2]). All methods use the same initial state flavor tag but they use different techniques to reconstruct the B decay and tag its final state flavor. The data consists of some 350,000 hadronic Z^0 decays collected with the upgrade vertex detector (VXD3) during the 1997-98 data taking. The analyses exploit the large longitudinal polarization of the electron beam, $P_e = (72.9 \pm 0.4)\%$ for 1997-98, to enhance the initial state tag.

2 Detector, Simulation and Event Selection

The components of the SLD detector relevant to this analysis are presented here. The Liquid Argon Calorimeter (LAC) was used for triggering, event shape measurement and electron identification. It provides excellent solid-angle coverage ($|\cos\theta| < 0.84$ and $0.82 < |\cos\theta| < 0.98$ in the barrel and endcap regions, respectively). The LAC is divided longitudinally into electromagnetic and hadronic sections. The energy resolution for electromagnetic showers is measured to be $\sigma/E = 15\%/\sqrt{E(GeV)}$, whereas that for hadronic showers is estimated to be $60\%/\sqrt{E(GeV)}$. The Warm Iron Calorimeter (WIC) provides efficient muon identification for $|\cos\theta| < 0.60$. Tracking is provided by the Central Drift Chamber (CDC)[3] for charged track reconstruction and momentum measurement and the CCD pixel Vertex Detector (VXD)[4] for precise position measurements near the interaction point. These systems are immersed in the 0.6 T field of the SLD solenoid. Charged tracks reconstructed in the CDC are linked with pixel clusters in the VXD by extrapolating each track and selecting the best set of associated clusters[3]. The track impact parameter resolutions at high momenta are 9 μm and 11 μm in the $r\phi$ and rz projections respectively (z points along the beam direction), while multiple scattering contributions are 33 μm $/(p\sin^{3/2}\theta)$ in both projections (where the momentum p is expressed in GeV/c).

The centroid of the micron-sized SLC Interaction Point (IP) in the $r\phi$ plane is

reconstructed with a measured precision of $\sigma_{IP} = (4 \pm 2)\,\mu$m using tracks in sets of ~ 30 sequential hadronic Z^0 decays. The median z position of tracks at their point of closest approach to the IP in the $r\phi$ plane is used to determine the z position of the Z^0 primary vertex on an event-by-event basis. A precision of $\sim 30\,\mu$m on this quantity is estimated using the $Z^0 \to b\overline{b}$ Monte Carlo (MC) simulation.

The simulated $Z^0 \to q\,\overline{q}$ events are generated using JETSET 7.4 [5]. The B meson decays are simulated using the CLEO B decay model [6] tuned to reproduce the spectra and multiplicities of charmed hadrons, pions, kaons, protons and leptons as measured at the Υ(4S) by ARGUS and CLEO [7]. Semileptonic decays follow the ISGW model [8] including 23% D^{**} production. The branching fractions of the charmed hadrons are tuned to the existing measurements [9]. The B mesons and b-baryons are generated with lifetimes of $\tau_{B^+} = 1.64$ ps, $\tau_{B^0} = 1.55$ ps, $\tau_{B_s^0} = 1.57$ ps, and $\tau_{\Lambda_b} = 1.22$ ps. The b-quark fragmentation follows the Peterson *et al.* parameterization [10]. Finally, the SLD detector is simulated using GEANT 3.21 [11].

Hadronic Z^0 event selection requires at least 7 CDC tracks which pass within 5 cm of the IP in z at the point of closest approach to the beam and which have momentum transverse to the beam direction $p_\perp > 200$ MeV/c. The sum of the energy of the charged tracks passing these cuts must be greater than 18 GeV. These requirements remove background from $Z^0 \to l^+l^-$ events and two-photon interactions. In addition, the thrust axis determined from energy clusters in the calorimeter must have $|\cos\theta_T| < 0.85$, within the acceptance of the vertex detector. These requirements yield a sample of $\sim 270,000$ hadronic Z^0 decays.

Good quality tracks used for vertex finding must have a CDC hit at a radius$<$39 cm, and have $\geq$23 hits to insure that the lever arm provided by the CDC is appreciable. The CDC tracks must have $p_\perp > 250$ MeV/c and extrapolate to within 1 cm of the IP in $r\phi$ and within 1.5 cm in z to eliminate tracks which arise from interaction with the detector material. The fit of the track must satisfy χ^2/d.o.f.< 8. Tracks must have at least two VXD links, and the combined CDC/VXD fit must also satisfy χ^2/d.o.f.< 8.

Both analyses make use of the inclusive topological vertexing technique [12] developed for B lifetime [13] and R_b [14] analyses to tag and reconstruct b-hadron decays. Secondary vertices are found in 65% of b hemispheres but in only 20% of c hemispheres and in less than 1% of uds hemispheres. The b purity of the sample is increased by reconstructing the vertex mass M, which includes a partial correction for missing decay products (see Ref. [3]). Requiring $M > 2$ GeV/c^2 yields a b-hadron sample with 98% b purity and 50% efficiency (for normalized decay length $> 5\sigma$). This inclusive vertexing technique has been adapted for semileptonic decays to reconstruct the D decay topology (see below).

3 Initial State Flavor Tagging

The large forward-backward asymmetry for $Z^0 \to b\,\overline{b}$ decays is used as a tag of the initial state flavor. The polarized forward-backward asymmetry $\tilde{A}_{FB}$ can be described by

$$\tilde{A}_{FB} = 2A_b\,\frac{A_e - P_e}{1 - A_eP_e}\,\frac{\cos\theta_T}{1+\cos^2\theta_T}\ , \tag{1}$$

where $A_b = 0.935$ and $A_e = 0.150$ (Standard Model values), P_e is the electron beam longitudinal polarization, and θ_T is the angle between the thrust axis and the electron beam direction (the thrust axis is signed such that it points in the same hemisphere as the reconstructed B vertex). Thus, left- (right-)polarized electrons tag b ($\bar{b}$) quarks in the forward hemisphere, and $\bar{b}$ (b) quarks in the backward hemisphere. Averaged over our acceptance, this yields an average correct tag probability of 0.74 for an average electron polarization $P_e = 73\%$. The probability for correctly tagging a b quark at production is expressed as

$$P_A(b) = \frac{1 + \tilde{A}_{FB}}{2} \ . \tag{2}$$

A jet charge technique is used in addition to the polarized forward-backward asymmetry. For this tag, tracks in the hemisphere opposite that of the reconstructed vertex are selected. These tracks are required to have momentum transverse to the beam axis $p_\perp > 0.15$ GeV/c, total momentum $p < 50$ GeV/c, impact parameter in the plane perpendicular to the beam axis $\delta < 2$ cm, distance between the primary vertex and the track at the point of closest approach along the beam axis $\Delta z < 10$ cm, and $|\cos\theta| < 0.87$. With these tracks, an opposite hemisphere momentum-weighted track charge is defined as

$$Q_{opp} = \sum_i q_i \left| \vec{p}_i \cdot \hat{T} \right|^\kappa \ , \tag{3}$$

where q_i is the electric charge of track i, $\vec{p}_i$ its momentum vector, $\hat{T}$ is the thrust axis direction, and κ is a coefficient chosen to be 0.5 to maximize the separation between b and $\overline{b}$ quarks. The probability for correctly tagging a b quark in the initial state of the vertex hemisphere can be parameterized as

$$P_Q(b) = \frac{1}{1 + e^{\alpha Q_{opp}}} \ , \tag{4}$$

where the coefficient $\alpha = -0.27$, as determined using the Monte Carlo simulation. This technique yields an average correct tag probability of 0.65 and is independent of the polarized forward-backward asymmetry tag.

Finally, the tag is further enhanced by the addition of other flavor-sensitive quantities from the hemisphere opposite that of the selected vertex. For this purpose, the inclusive topological vertexing technique mentioned earlier is used. The sensitive variables are: the total track charge and charge dipole of a topologically reconstructed vertex, the charge of a kaon identified in the Cherenkov Ring Imaging Detector, and the charge of a lepton with high transverse momentum with respect to the direction of the nearest jet. The addition of these tags improves the average correct tag probability by about 0.03.

The various tags are combined to form an overall initial state tag characterized by a b-quark probability P_i. The average correct tag probability is 0.80 with full efficiency. Fig. 1 shows the P_i distributions for data and Monte Carlo in the Charge Dipole analysis (see below for a description of the analysis), and also indicates the clear separation between b and $\overline{b}$ quarks.

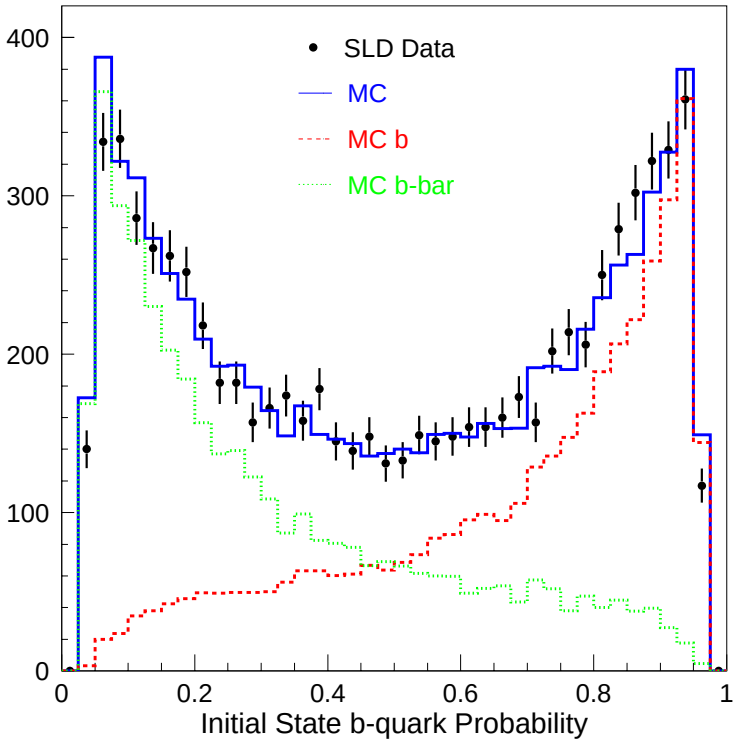

Figure 1: *Distribution of the computed initial state b-quark probability for data (points) and Monte Carlo (histograms) showing the b and $\bar{b}$ components for the events selected in the Charge Dipole analysis.*

4 Lepton+D Analysis

The lepton+"D" analysis aims at reconstructing the B and D vertex topologies of semileptonic B decays. It proceeds by first selecting event hemispheres containing an identified lepton (e or μ) with $|\cos\theta| < 0.7$. Then, a D vertex candidate is reconstructed using a similar topological technique as that described earlier. This vertex is constrained to lie near the plane containing the lepton track and the IP, and to be downstream of the lepton, thereby reducing the confusion between primary and secondary tracks and thus allowing efficient reconstruction of semileptonic B decays at short decay lengths. Several cuts are added to clean up the D vertex candidate and reduce the contamination from cascade ($b \to c \to l$) charm semileptonic decays. The cuts are as follows: the lepton momentum transverse to the D trajectory $p_T > 0.9$ GeV/c, the invariant mass of all D vertex tracks (assumed to be pions) is less than 1.95 GeV/c^2 and the sum of all track charges at the D vertex is ≤ 1 in absolute value. An additional requirement aimed at suppressing the ($b \to c \to l$) contribution is that either the χ^2 for fitting the lepton and D vertex tracks to a single vertex is larger than that obtained for the D vertex tracks alone or the invariant mass of the lepton + D vertex tracks is greater than 2.5 GeV/c^2. Furthermore, the difference in the mass between the $D+l$ and the D tracks alone is greater than 0.6 GeV/c^2. The B decay vertex is reconstructed by intersecting the lepton and D trajectories. For

this analysis, only vertices with positive reconstructed decay length are selected.

To enhance the fraction of B_s^0 decays, the sum of lepton + D vertex track charges is required to be $Q = 0$. This enhances the B_s^0 fraction to 15.9% of all b hadrons in the $Z^0 \to b\overline{b}$ MC (the B_s^0 production fraction in the $Z^0 \to b\overline{b}$ MC is 10.8%). Although the analysis described above achieves good b-hadron purity, an additional reduction in the non-b background is achieved at only a small cost in efficiency by applying an event b tag: the event should contain either at least one hemisphere with an inclusive topological vertex with $M > 1.6$ GeV/c^2 or a minimum of 2 tracks with positive 3-D impact parameter greater than 3 σ. As a result, the $udsc$ contamination is reduced from 4.3% to 1.2% in the final sample.

A sample of 2009 decays is thus obtained in the 1997-98 data. Various comparisons between data and Monte Carlo simulation were performed which generally showed good agreement. For example, Fig. 2 shows the distributions of lepton momentum transverse

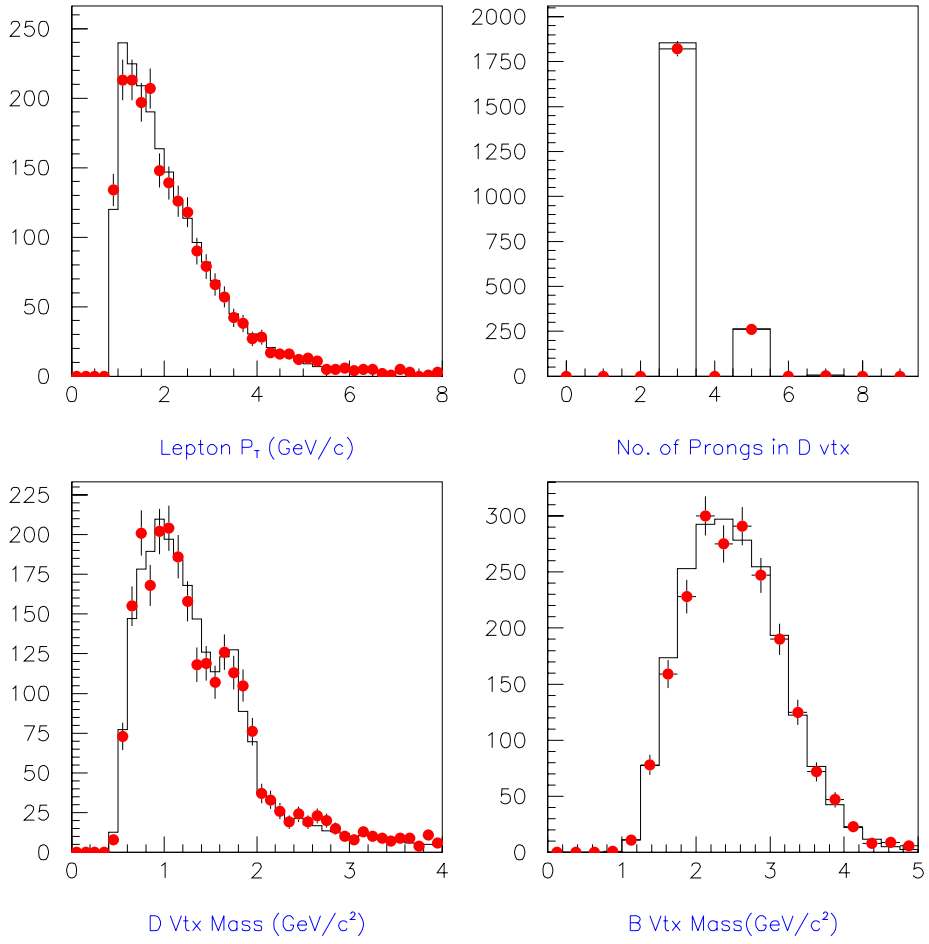

Figure 2: *Distributions of lepton momentum transverse to the D vertex trajectory, D vertex track multiplicity, D vertex mass (with the cut on the mass removed) and lepton+D vertex mass for data (points) and Monte Carlo (histograms).*

to the D vertex trajectory, D vertex track multiplicity, and invariant mass of all tracks in the D vertex and (assuming all tracks are pions) as well as in both B and D vertices.

A powerful check of the analysis and the purity of the final state tag is the polarization-dependent forward-backward asymmetry shown in Fig. 3. A clear asymmetry is observed, in reasonable agreement with the Monte Carlo, indicating that the final state tag purity is adequately modeled in the simulation.

The study of the time dependence of B_s^0–$\overline{B_s^0}$ mixing requires a precise determination of the B decay proper time $t = L/(\gamma\beta c)$, where L is the reconstructed decay length (distance between the IP and the B vertex) and $\gamma\beta = p_B/m_B$ is computed from the estimated B momentum p_B and the known mass of the B meson, m_B. Reconstruction of the b-hadron boost uses both tracking and calorimeter information. A detailed description of the reconstruction algorithm may be found in Ref. [15]. The overall performance of the decay length and boost measurements for B_s^0 decays proceeding via the direct ($b \to l$) transition is shown in Fig. 4. The proper time distribution is shown in Fig. 5.

The final state B^0 or $\overline{B^0}$ flavor is tagged by the sign of the lepton charge. Each decay is assigned a final state b-quark probability P_f, defined such that $P_f > 0.5$ (< 0.5) corresponds to a negatively (positively) charged lepton which then tags the decay as $\overline{B}$ (B). The magnitude of the correct tag probability depends on the sample composition as well as on the lepton p_T. The lepton sources in selected B_s^0 decays are as follows: 86.5% ($b \to l^-$), 6.0% ($b \to c \to l^+$), 1.9% ($b \to \bar{c} \to l^-$), 1.5% ($b \to X^-$) (right-sign misidentified lepton), 0.9% ($b \to X^+$) (wrong-sign misidentified lepton), 1.9% ($b \to$ other $\to l^-$), and 1.1% ($b \to$ other $\to l^+$). The final state correct tag probability is thus 0.918. Further enhancement of the tag is achieved by taking into account the strong p_T dependence of the various lepton source fractions. At high p_T the correct tag probability for B_s^0 decays increases to 0.953.

4.1 Likelihood Analysis

The search for the time dependence of B_s^0–$\overline{B_s^0}$ mixing is carried out with a likelihood analysis which includes the effect of detector smearing, mistag of both initial and final states, selection efficiencies and the dependence on the oscillation frequency Δm_s. The probability that a meson created as a B_s^0 ($\overline{B_s^0}$) will decay as a B_s^0 ($\overline{B_s^0}$) after proper time t can be written as

$$P_u(t) = \frac{\,}{2}\, e^{-\Gamma t}\, [1 + \cos(\Delta m_s\, t)] \ , \tag{5}$$

where Δm_s is the mass difference between the mass eigenstates, , is the average decay width of the two states and P_u denotes the probability to remain 'unmixed'. The effects of CP violation are assumed to be small and are neglected. Similarly, the probability that the same initial state will 'mix' and decay as its antiparticle is

$$P_m(t) = \frac{\,}{2}\, e^{-\Gamma t}\, [1 - \cos(\Delta m_s\, t)] \ . \tag{6}$$

Decays are tagged as mixed or unmixed if the product $(P_i - 0.5) \times (P_f - 0.5)$ is smaller or greater than 0, respectively. The probability for a decay to be in the mixed

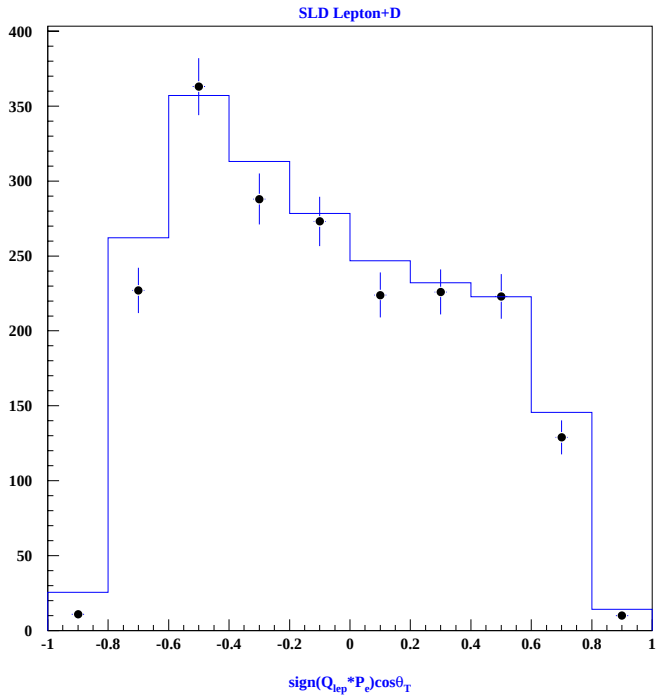

Figure 3: *Distribution of* $\cos\theta$ *for the thrust axis direction signed by the product* $(Q_{lept} \times P_e)$ *for data (points) and Monte Carlo (histograms).*

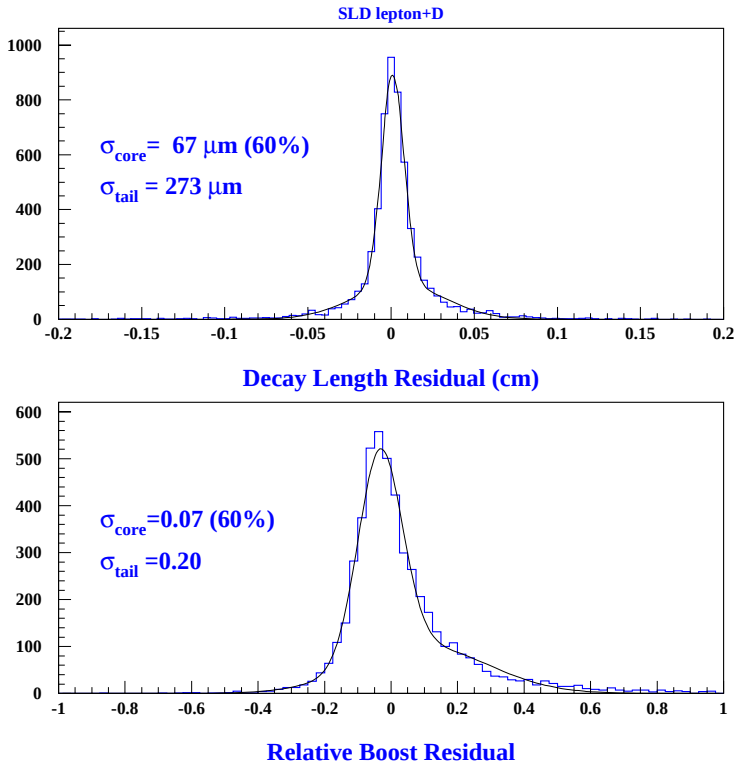

Figure 4: *Distributions of the decay length and relative boost residuals for* B_s^0 $(b \to l)$ *decays in the simulation.*

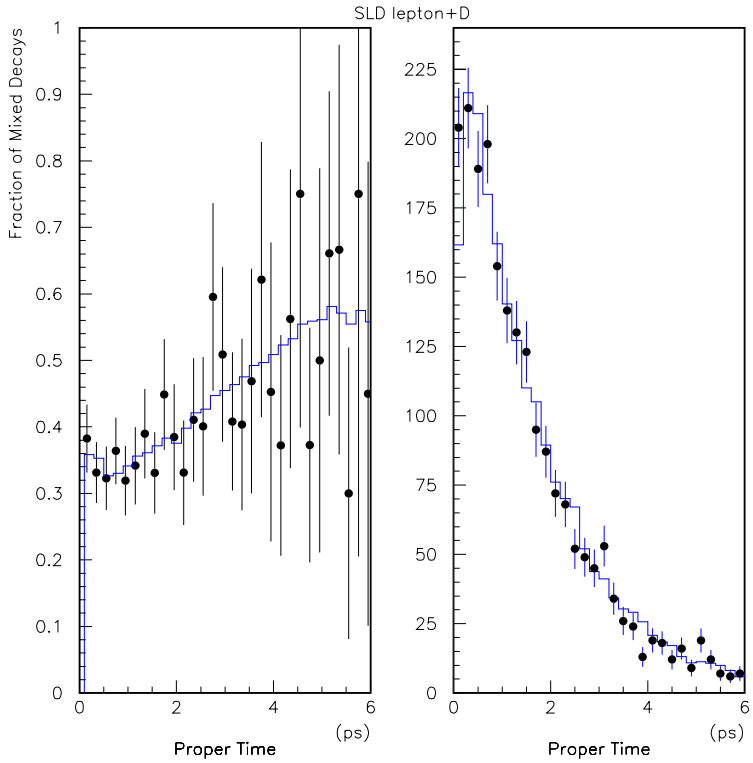

Figure 5: *Distributions of the fraction of decays tagged as "mixed" (left) and reconstructed proper time (right) for the data (points) and the likelihood function (histograms).*

sample is expressed as:

$$\begin{aligned}
\mathcal{P}_{mixed}(t,\Delta m_s) \;=\; & f_u \frac{e^{-t/\tau_u}}{\tau_u}\,\eta_u \\
& + \frac{f_d}{2}\frac{e^{-t/\tau_d}}{\tau_d}\left[\eta_d(1+\cos\Delta m_d t)+(1-\eta_d)(1-\cos\Delta m_d t)\right] \\
& + \frac{f_s}{2}\frac{e^{-t/\tau_s}}{\tau_s}\left[\eta_s(1+\cos\Delta m_s t)+(1-\eta_s)(1-\cos\Delta m_s t)\right] \\
& + f_\Lambda \frac{e^{-t/\tau_\Lambda}}{\tau_\Lambda}\,\eta_\Lambda \\
& + \frac{f_{udsc}}{2}\,F_{udsc}(t),
\end{aligned}$$

where f_j represents the fraction of each b-hadron type and background ($j = u, d, s, \Lambda, udsc$ correspond to B^+, B^0_d, B^0_s, b-baryon, and $udsc$ background), τ_j and η_j are the lifetime and mistag probability for b hadrons of type j, and $F_{udsc}(t)$ is a function describing the proper time distribution of the $udsc$ background (a sum of two exponentials is used). A similar expression for the probability $\mathcal{P}_{unmixed}$ to observe a decay tagged as unmixed is obtained by replacing the mistag rate η by $1-\eta$.

Detector and vertex selection effects are introduced by convoluting the above probability functions with a proper time resolution function $\mathcal{R}(T,t)$ and a time-dependent efficiency function $\varepsilon(t)$:

$$P_{mixed}(T,\Delta m_s) = \int_0^\infty \mathcal{P}_{mixed}(t,\Delta m_s)\ \mathcal{R}(T,t)\ \varepsilon(t)\ dt\ , \tag{7}$$

where t is the "true" time and T is the reconstructed time. Again, a similar expression applies to the unmixed probability $P_{unmixed}$. The resolution function is parameterized by the sum of two Gaussians:

$$\begin{aligned}\mathcal{R}(T,t) &= f_1\ \frac{1}{\sigma_1(t)\sqrt{2\pi}}\ e^{-\frac{1}{2}\left(\frac{T-t}{\sigma_1(t)}\right)^2} \\ &\quad + f_2\ \frac{1}{\sigma_2(t)\sqrt{2\pi}}\ e^{-\frac{1}{2}\left(\frac{T-t}{\sigma_2(t)}\right)^2}\ ,\end{aligned}$$

where the fraction f_1 is set to 60% and $f_2 = 1 - f_1$. The proper time resolution is a function of proper time and also depends on the measured boost $\gamma\beta$, its resolution $\sigma_{\gamma\beta}$ and on the estimate of the decay length resolution σ_L:

$$\sigma(t) = \left[\left(\frac{\sigma_L}{\gamma\beta c}\right)^2 + \left(t\,\frac{\sigma_{\gamma\beta}}{\gamma\beta}\right)^2\right]^{1/2}\ . \tag{8}$$

For each decay, the resolution σ_L is computed from the vertex fit and IP position measurement errors, with a scale factor determined using the MC simulation (the scale factor is introduced mostly to account for the fact that the analysis does not attempt to fully reconstruct the D meson decay). The relative boost residual $\sigma_{\gamma\beta}/\gamma\beta$ is parameterized as a function of the lepton + D vertex total track energy, with parameters extracted from the MC simulation. Similarly, the efficiency $\varepsilon(t)$ is parameterized using the MC simulation. All parameterizations are performed separately for each b-hadron type. For example, the efficiency for B_s^0 decays is given by

$$\varepsilon(t) = a\ \frac{1-e^{bt}}{1+e^{bt}} + c + dt\ , \tag{9}$$

with $a = 0.018$, $b = -14.3$, $c = -0.0008$, and $d = -0.0006$. Furthermore, σ_L and $\sigma_{\gamma\beta}$ resolutions are handled separately for the main lepton sources $(b \to l)$, $(b \to c(\bar{c}) \to l)$ and $(b \to X)$. As a consequence, different resolution functions are used for the different sources and the expressions for P_{mixed} and $P_{unmixed}$ are modified accordingly.

The study of the time dependence of B_s^0–$\overline{B_s^0}$ mixing is carried out using the amplitude method described in Ref. [16]. Instead of fitting for Δm_s directly, the analysis is performed at fixed values of Δm_s and a fit to the amplitude A of the oscillation is performed, i.e. in the expression for the mixed and unmixed probabilities, one replaces $[1 \pm \cos(\Delta m_s t)]$ with $[1 \pm A\cos(\Delta m_s t)]$. This method is similar to Fourier transform analysis and has the advantage of facilitating the combination of results from different analysis techniques and different experiments.

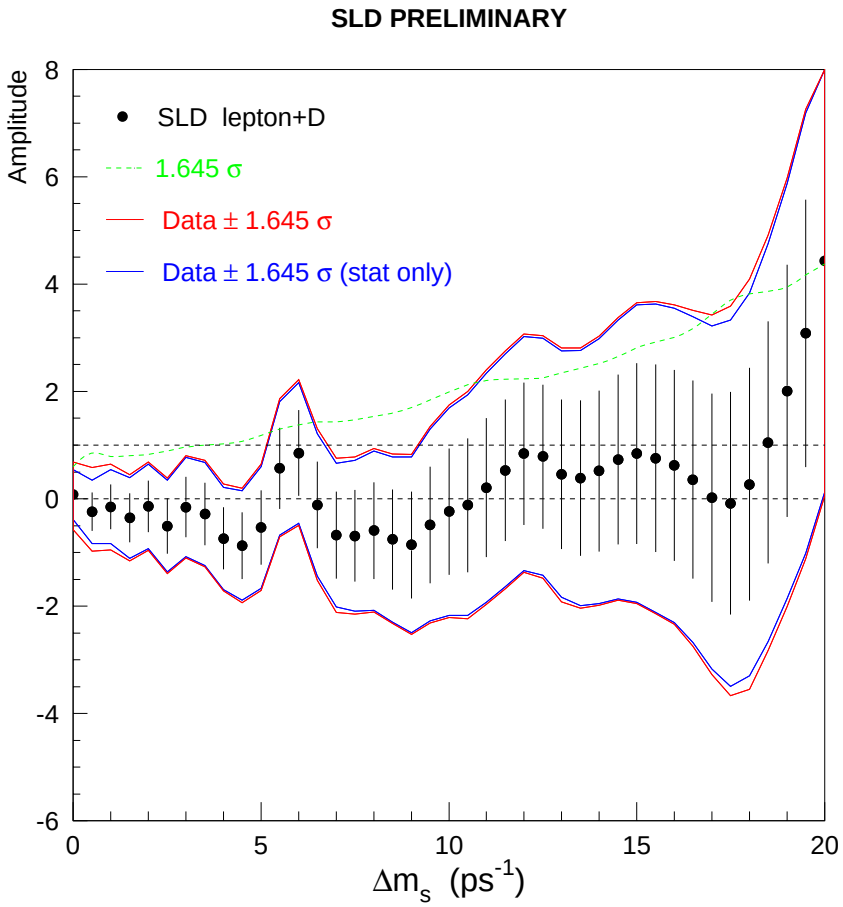

Figure 6: *Measured amplitude as a function of Δm_s in the lepton+D analysis.*

The measured amplitude for the lepton+D analysis is shown as a function of Δm_s in Fig. 6. The measured values are consistent with $A = 0$ for the whole range of Δm_s up to 20 ps^{-1} and no evidence is found for a preferred mixing frequency.

Systematic uncertainties have been computed following Ref. [16] and are summarized in Table 1 for several Δm_s values. Uncertainties in the sample composition are estimated by varying the fraction of $udsc$ background by $\pm 20\%$ and the production fractions of B_s^0 and b-baryons according to 0.108 ± 0.014 and $0.102^{+0.023}_{-0.021}$, respectively. Other physics modeling uncertainties are $\tau(B^+) = 1.64 \pm 0.04$ ps, $\tau(B_d^0) = 1.55 \pm 0.04$ ps, $\tau(B_s^0) = 1.57 \pm 0.06$ ps, $\tau(\Lambda_b) = 1.22 \pm 0.06$ ps, and $\Delta m_d = 0.480 \pm 0.020$ ps^{-1}. Uncertainties in the modeling of the detector include $\pm 10\%$ and $\pm 20\%$ variations in decay length and boost resolutions, respectively. Initial state tag uncertainties are estimated by varying the correct tag probability by ± 0.02 (i.e., a $\pm 10\%$ variation of the mistag rate), corresponding to the expected contribution from uncertainties in the measured electron beam polarization, the value of A_b, and the self-calibrated jet charge analyzing power. Final state tag uncertainties include a $\pm 15\%$ variation in the lepton misidentification rate, as well as the effect of uncertainties in the branching ratios $\mathcal{B}(b \to l) = 0.112 \pm 0.002$, $\mathcal{B}(b \to \bar{c} \to l) = 0.016 \pm 0.004$, and $\mathcal{B}(b \to c \to l) = 0.080 \pm 0.004$. The dominant uncertainty is the B_s^0 production fraction in $Z^0 \to b\overline{b}$ events.

Table 1: Measured values of the oscillation amplitude A with a breakdown of systematic uncertainties for several Δm_s values in the lepton+D analysis.

Δm_s	5 ps^{-1}	10 ps^{-1}	15 ps^{-1}
Measured amplitude A	-0.535	-0.238	0.841
σ_A^{stat}	± 0.689	± 1.175	± 1.685
σ_A^{syst}	$^{+0.203}_{-0.168}$	$^{+0.288}_{-0.217}$	$^{+0.301}_{-0.187}$
$f_s = \mathcal{B}(b \to B_s^0)$	$^{-0.149}_{+0.192}$	$^{-0.178}_{+0.250}$	$^{-0.135}_{+0.198}$
$f_\Lambda = \mathcal{B}(b \to b\text{−baryon})$	$^{+0.035}_{-0.033}$	$^{+0.063}_{-0.041}$	$^{+0.049}_{-0.029}$
$udsc$ fraction	$^{+0.019}_{-0.020}$	$^{-0.014}_{+0.031}$	$^{-0.021}_{+0.049}$
decay length resolution	$^{-0.002}_{+0.002}$	$^{+0.069}_{-0.044}$	$^{+0.112}_{-0.109}$
boost resolution	$^{+0.009}_{-0.034}$	$^{-0.046}_{-0.055}$	$^{+0.160}_{+0.009}$
b-hadron lifetimes	$^{+0.017}_{-0.021}$	$^{+0.056}_{-0.053}$	$^{+0.048}_{-0.043}$
Δm_d	$^{-0.015}_{+0.012}$	$^{-0.001}_{+0.022}$	$^{+0.014}_{+0.006}$
initial state tag	$^{+0.029}_{-0.034}$	$^{+0.031}_{-0.006}$	$^{+0.050}_{-0.023}$
$\mathcal{B}(b \to l)$, $\mathcal{B}(b \to \bar{c} \to l)$, $\mathcal{B}(b \to c \to l)$	$^{+0.038}_{-0.042}$	$^{+0.077}_{-0.059}$	$^{+0.055}_{-0.030}$
lepton misidentification	$^{-0.003}_{+0.005}$	$^{+0.004}_{+0.015}$	$^{+0.006}_{+0.015}$

5 Vertex Charge Dipole Analysis

The Charge Dipole analysis aims at reconstructing the B and D vertex topologies in inclusive decays and tags the B^0 or $\overline{B^0}$ decay flavor based on the charge difference between the B and D vertices. This analysis technique is unique to SLD and relies extensively on the excellent resolution of the vertex detector.

In the following, we first describe a new algorithm used to identify primary, secondary and tertiary vertices, then discuss details of the B_s^0–$\overline{B_s^0}$ mixing analysis.

5.1 Ghost Track Algorithm

The B decay flavor tag with the charge dipole relies on the kinematic fact that the boost of the B decay system carries the cascade charm decay downstream from the B decay vertex. Monte Carlo studies show that in B decays producing a single D meson the cascade D decays on average 4200 μm from the IP, while the intermediate B vertex is displaced on average only 46 μm transversely from the line joining the IP to the D decay vertex. This kinematic stretching of the B decay chain into an approximately straight line is exploited by the ghost track algorithm. This new algorithm has two stages and operates on a given set of selected tracks in a jet or hemisphere. First, the best estimate of the straight line from the IP directed along the B decay chain is found. This line is promoted to the status of a track by assigning it a finite width. This new track, regarded as the resurrected image of the deceased B hadron, is called the "ghost" track. Secondly, the selected tracks are vertexed with the ghost track and the IP to build up the decay

chain along the ghost direction. Both stages are now described in more detail.

Given a set of tracks in a hadronic jet or hemisphere a new track G is created with the properties that it is a straight line from the IP directed along the jet or thrust axis and has a constant resolution width of 25 μm in both $r\phi$ and rz. For each track i a vertex is formed with track G and the vertex location $\mathbf{r_i}$, fit χ^2_i and L_i are determined (L_i is the longitudinal displacement from the IP of $\mathbf{r_i}$ projected onto the direction of track G). This is calculated for each of the tracks and the summed χ^2 is formed:

$$\chi^2_S = \sum_i \begin{array}{ll} \chi^2_i & \mathrm{L}_i \geq 0.0 \\ (2\chi^2_{0i} - \chi^2_i) & \mathrm{L}_i < 0.0 \end{array} \tag{10}$$

where χ^2_{0i} is the χ^2_i of track i to track G determined at $\mathrm{L}_i = 0$ rather than at the best fit vertex location. The aim is to construct this quantity, χ^2_S, such that when the direction of G is varied the minimum of χ^2_S provides the best estimate of the B decay direction. If the initial direction is a relatively long way from the B line of flight, some or all of the decay tracks may vertex with G with a negative value of L_i. In this case the $2\chi^2_{0i} - \chi^2_i$ term above helps to push track G towards the B flight path as χ^2_S is minimized. This first minimization using equation 10 is designed for this purpose. (Note that the contribution of each track as χ^2_S is minimized changes in a continuous manner even if L_i changes sign since $\chi^2_i = \chi^2_{0i}$ at $\mathrm{L}_i = 0$.)

The value of χ^2_S is recalculated as track G is rotated (about the pivot at the IP) incrementally in ever decreasing angular steps $\delta\theta$ and $\delta\phi$ until the minimum is found within the required precision (< 0.1 mrad, i.e. within 1 μm at 1 cm from the IP). The width of track G is set such that the maximum $\chi^2_i = 1.0$ for all tracks with $\mathrm{L}_i > 0$ (if this is less than 25μm, it is restored to 25μm). The track G is now consistent with all potential B decay candidate tracks ($\mathrm{L}_i > 0$) at the level $\chi^2_i \leq 1.0$. In other words, the new width of G measures the degree to which the tracks conform to a straight line decay chain. A second iteration in $\delta\theta$,$\delta\phi$ now takes place with the summed χ^2 redefined as:

$$\chi^2_S = \sum_i \begin{array}{ll} \chi^2_i & \mathrm{L}_i \geq 0.0 \\ \chi^2_{0i} & \mathrm{L}_i < 0.0 \end{array} \tag{11}$$

which is not sensitive to any spurious background track with a negative value of L_i which might otherwise perturb the direction of track G. After finding the new minimum of χ^2_S the width of G is again recalculated such that $\chi^2_i \leq 1.0$ for all tracks i with $\mathrm{L}_i > 0$. Again this width is required to be at least 25 μm. Track G is now directed along the best guess of the B decay line of flight and has a width such that it is consistent with potential B decay tracks in the jet, track G is now called the "ghost" track.

The second stage of the algorithm begins by defining a fit probability for a set of tracks to form a vertex with each other and with the ghost track (or IP). This probability then measures the likelihood of the set of tracks both belonging to a common vertex *and* being consistent with the ghost track (or IP) and hence forming a part of the B decay chain. These probabilities are determined from the fit χ^2 which is in turn determined algebraically from the parameters of the selected tracks and the ghost track (or the $7 \times 7 \times 30\mu\mathrm{m}^3$ ellipsoid assumed for the IP). The earlier requirement that each $\mathrm{L}_i > 0$ track makes a $\chi^2_i \leq 1.0$ with the ghost track has the effect that the fit probabilities have the

desired property of having an approximately flat distribution from 0.0 to 1.0 for genuine vertices, independent of both multiplicity and decay length. This property also relies on the choice of the number of degrees of freedom as 2N−2 (or 2N) when fitting N tracks together with the ghost track (or IP). Fake vertices peak at probability close to 0.0.

For a set of N tracks, there are initially N+1 candidate vertices (N 1-prong secondary vertices and a bare IP). A matrix of track i – track j associations is constructed to store the calculated probabilities of each candidate vertex pair fitted together with the ghost track. A further column and row is added to the matrix to store the probabilities of each track fit with the IP ellipsoid. The upper triangle of the matrix (i.e. the ij $(i < j)$ elements) stores the probabilities while the lower triangle (initialized with ij $(i > j)$ elements set to 0.0) indelibly records which tracks (and IP) have been assigned together in a common vertices as the algorithm progresses. Once the upper triangle has been filled, the highest probability in the matrix table is found and the corresponding candidate vertex pair are from then on tied together in a new candidate vertex for all future computations by flagging the corresponding lower triangle elements of the matrix with non-zero values. The upper triangle of the matrix is now refilled taking into account the associations that have so far been made, the new maximum probability is found, and the corresponding subset of the tracks and IP is tied together. At each iteration of combining the maximum probability matrix element contributors, the number of candidate vertices decreases by one. The iterations continue until the maximum probability is less than 1%. At this point the tracks and IP have been divided into unique subsets by the associations thereby defining topological vertices.

Jets or hemispheres in which three vertices are found – the primary (which includes by definition the IP), a secondary and a tertiary – are used for the charge dipole analysis. The secondary vertex is identified as the B decay vertex and the tertiary as the cascade charm decay. As well as improving the purity and efficiency of the dipole reconstruction (by requiring the vertices be consistent with a single line of flight) the ghost track algorithm has the additional advantage of allowing the direct reconstruction of 1-prong vertices, including the topology consisting of 1-prong B decay and D decays.

5.2 Event Selection

Hemispheres containing both a secondary and tertiary vertex are selected for the charge dipole analysis. Furthermore, the invariant mass computed using all secondary and tertiary vertex tracks is required to be $M > 2$ GeV/c^2 (the computed mass includes a partial correction for missing decay products) and the total track charge Q (from both secondary and tertiary vertices) is required to be 0 to enhance the fraction of B_s^0 decays in the sample and to increase the quality of the charge difference reconstruction for neutral B decays. As mentioned in the previous section, the (secondary) vertex that is closer to the IP is labelled "B" and that further away (tertiary) is labelled "D." A "Charge Dipole" is defined as $\delta Q \equiv D_{BD} \times SIGN(Q_D - Q_B)$, where D_{BD} is the distance between the two vertices and Q_B (Q_D) is the charge of the B (D) vertex. Positive (negative) values of δQ tag $\overline{B^0}$ (B^0) decays. Requirements on the vertices are: 250 μm $< D_{BD} <$ 1 cm, D vertex mass $<$ 2.0 GeV/c^2 (assuming all tracks are pions), B vertex decay length $L > 0$, $Q_B \neq Q_D$, "ghost" track width $< 300\mu$m and cosine between the B vertex-to-IP and

nearest jet axis directions < 0.9. MC studies indicate that, after these selection cuts, the track assignment to the B (D) vertex is 89% (86%) correct for decays containing one D meson in the final state. For all data and MC events, hemispheres already containing a vertex selected by the lepton+D or lepton+track analyses are removed such that the analyses are statistically uncorrelated. The *udsc* background is further suppressed by demanding that the event contains either an opposite hemisphere topological vertex with $M > 2$ GeV/c^2 or at least 3 tracks with positive 2-D impact parameter $> 3\,\sigma$. The *udsc* fraction is thus reduced to 2.1%.

Applying all the above cuts, a sample of 7547 decays is selected in the 1997-98 data. Figure 7 shows distributions of the B and D vertex track multiplicities, and distance and charge difference between B and D vertices in the selected sample. Good agreement between data and MC is obtained. A slight discrepancy in the D vertex track multiplicity is apparent but was determined to have negligible impact on the analysis. The B_s^0 fraction estimated from the $Z^0 \to b\overline{b}$ MC is 15.6%. Figure 8 displays the distribution of charge dipole δQ for the data sample and also indicates the separation between b hadrons containing b or $\bar{b}$ quarks in the MC.

The average correct tag probability for the charge dipole tag is 0.79 for selected B_s^0 decays and is parameterized as a function of decay length, as shown in Fig. 9. Furthermore, the correct tag probability depends on the charm content of the decay products. Thus, the correct tag probability is parameterized separately for B_d^0 and B_s^0 decays into five different final states: D^0X, D^+X, D_sX, charmed hadron X, and $D\overline{D}X$ (this last category also incorporates charmonium production, i.e. it includes all $b \to c\overline{c}s$ decays). For example, the correct tag probability is 0.91 for $B_s^0 \to D_sX$ decays but only 0.53 for $B_s^0 \to D\overline{D}X$ decays.

As hadronic decays of B mesons are not as well known as semileptonic decays, it is important to check the tag purity estimated using measured quantities like the polarization-dependent forward-backward asymmetry shown in Fig. 10. Good agreement with the MC is observed, indicating that the charge dipole tag purity is well modeled. It should be noted that this asymmetry is diluted by both initial and final state mistags and by B^0–$\overline{B^0}$ mixing. The dilution due to mixing can be reduced by selecting vertices with total charge $Q = \pm 1$, in which case a stronger asymmetry is observed (see Fig. 10). Another useful test of the charge dipole tag in B_d^0 decays is the measurement of the time dependence of B_d^0–$\overline{B_d^0}$ mixing. This has been checked using the full likelihood analysis described in the following section. Fitting for the B_d^0–$\overline{B_d^0}$ mixing frequency yields $\Delta m_d = 0.521 \pm 0.040$ ps^{-1} (statistical error only), see Fig. 11. This value agrees with the latest world average value of 0.471 ± 0.016 ps^{-1} [17]. The mixed fraction as a function of proper time is displayed in Fig. 12. The figure shows the expected degradation of the final state tag purity for decays at small proper time due to contamination from primary tracks in decays taking place near the IP.

5.3 Likelihood Analysis

The B_s^0–$\overline{B_s^0}$ mixing fit is done in a way similar to that used for the lepton+D analysis. Slight differences are as follows: for decay topologies consisting of a 1-prong B vertex plus a 1-prong D vertex, the decay length resolution σ_L does not use the vertex fit and

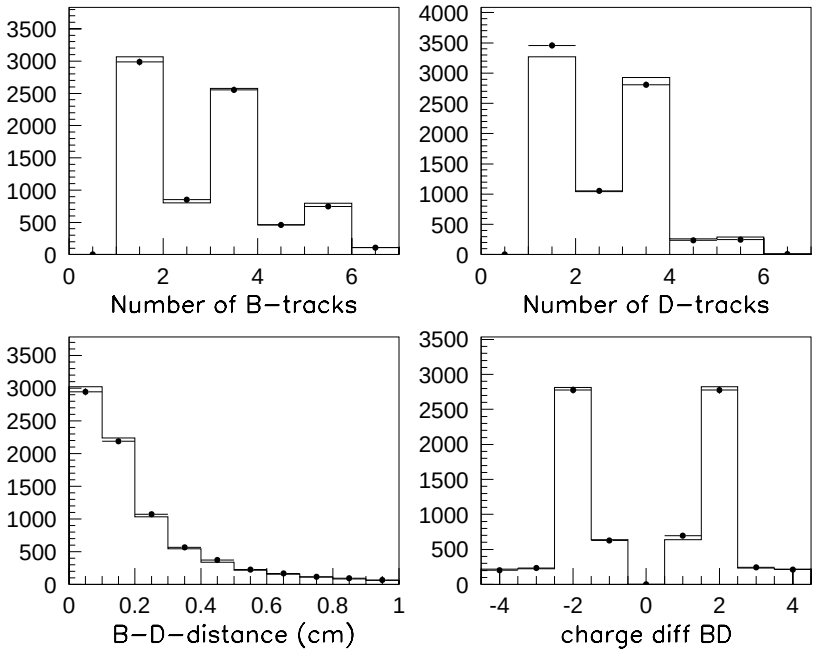

Figure 7: *Distributions of B and D vertex track multiplicity, as well as distance and charge difference between B and D vertices for data (points) and Monte Carlo (histograms) in the Charge Dipole analysis.*

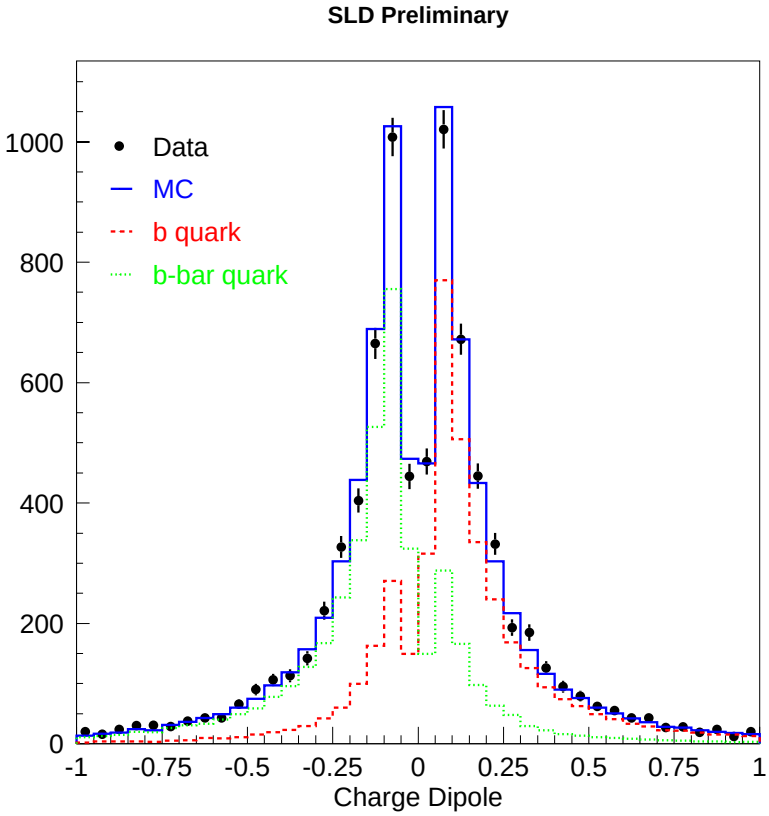

Figure 8: *Distribution of the charge dipole for data (points) and Monte Carlo (solid histogram). Also shown are the contributions from b hadrons containing a b quark (dotted histogram) or a $\bar{b}$ quark (dashed histogram).*

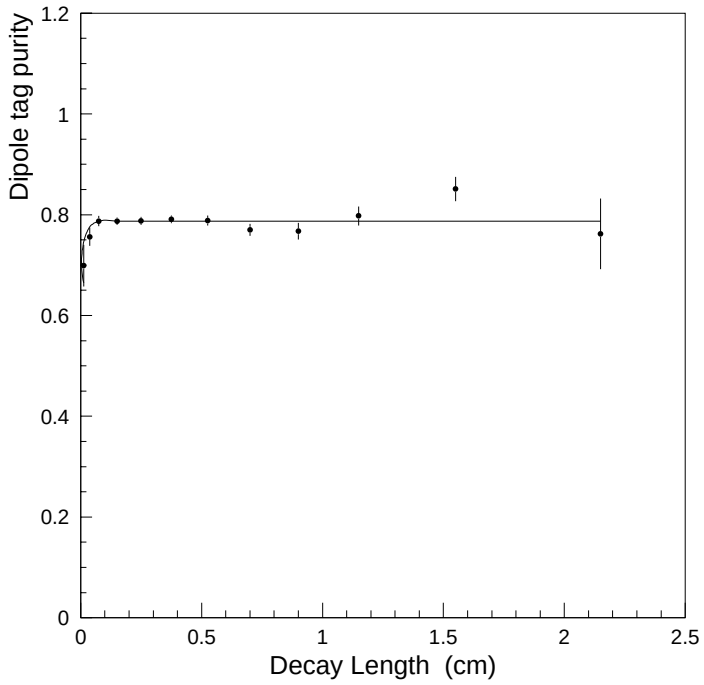

Figure 9: *Charge dipole tag purity as a function of reconstructed decay length in simulated* B_s^0 *decays. The function is the result of a fit.*

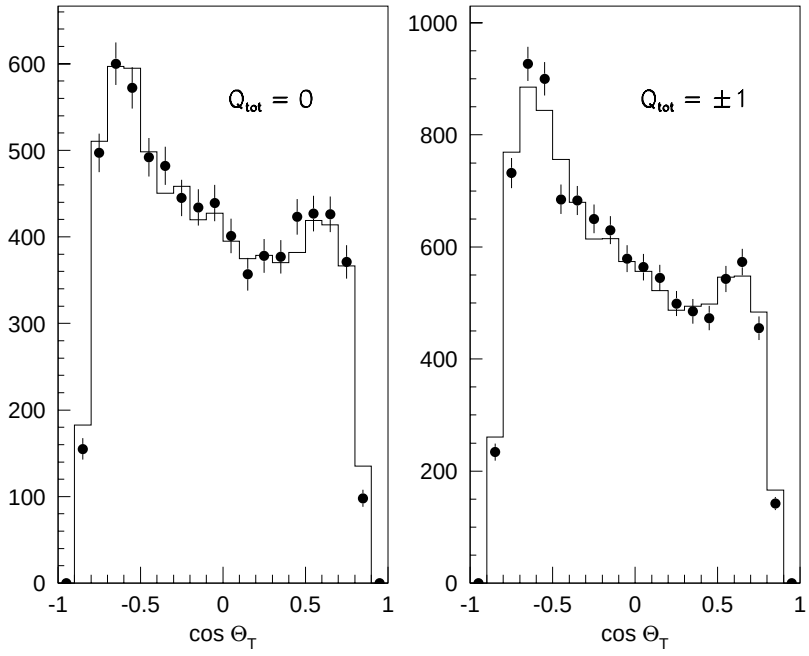

Figure 10: *Distributions of* $\cos\theta$ *for the thrust axis direction signed by the product* $(\delta Q \times P_e)$ *for data (points) and Monte Carlo (histograms) in subsamples with* $Q_{tot} = 0$ *and* $Q_{tot} = \pm 1$ *for the Charge Dipole analysis.*

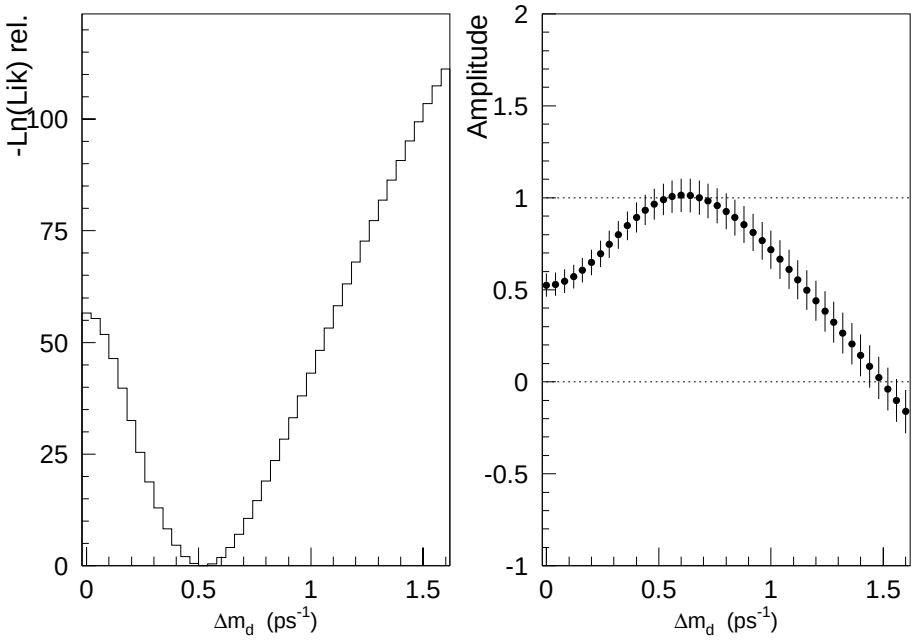

Figure 11: *Log likelihood as a function of Δm_d and measured amplitude as a function of Δm_d for the Charge Dipole analysis.*

IP position measurement errors but is extracted from the overall decay length residual distributions in the simulation. Furthermore, σ_L is parameterized separately for decays with right and wrong charge dipole tags as it was found that the resolution is considerably better for the correctly tagged decays (this is similar to differences in resolution between $(b \to l)$ and $(b \to c \to l)$ in the lepton+D analysis). For example, the average decay length resolution for B_s^0 decays with right (wrong) charge dipole tag can be parameterized by a sum of two Gaussians of widths $\sigma_{L1} = 87\,\mu$m ($123\,\mu$m) and $\sigma_{L2} = 368\,\mu$m ($614\,\mu$m), where the first Gaussian represents 60% of the decays. Decays reconstructed within $500\,\mu$m of the IP have worse decay length resolution and suffer from asymmetric tails (this is most likely due to the addition of a primary track in the secondary vertex). These effects have been taken into account in the analysis. The average relative boost residual for B_s^0 decays can be parameterized by a sum of two Gaussians of width $\sigma_{B1} = 0.08$ and $\sigma_{B2} = 0.26$, where the first Gaussian represents 60% of the decays. Offsets in the boost reconstruction, especially for decays with low reconstructed boost, have been corrected for as well.

As indicated above, the mistag rate as well as the decay length and boost resolutions of the main B_d^0 and B_s^0 decay channels are parameterized separately. Furthermore, the fraction of decays into each of the D^0X, D^+X, D_sX, charmed hadron X, and $D\overline{D}X$ final states is parametrized as a function of the vertex mass M since, in particular, Monte Carlo studies showed a significant dependence of the fraction of $D\overline{D}X$ final states upon M.

The result of the amplitude fit is displayed in Fig. 13. Systematic uncertainties are estimated as for the lepton+D analysis except for those affecting the final state tag. Here, uncertainties in the tag purity modeling are obtained by varying the following branching ratios: $\mathcal{B}(b \to c\bar{c}s) = 0.22 \pm 0.05$ and $\mathcal{B}(B \to D^0X) \pm 20\%$ (where X represents any particle

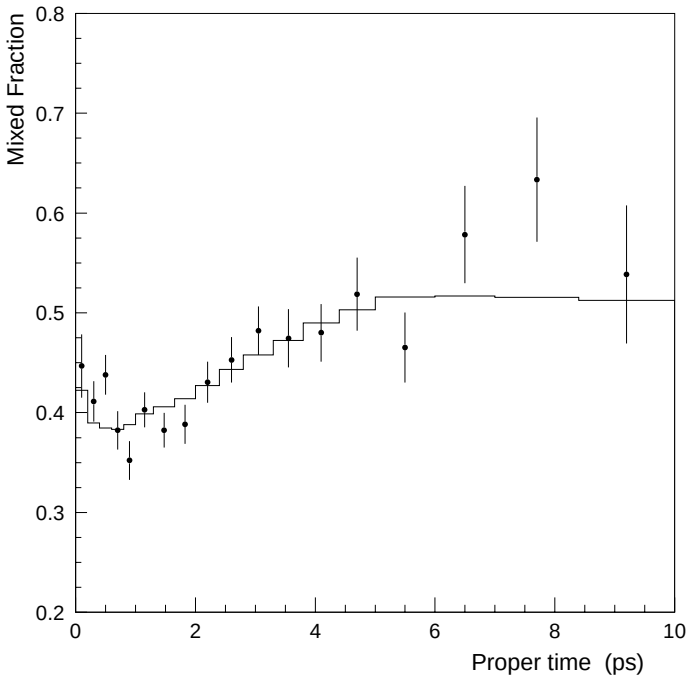

Figure 12: *Distributions of the fraction of decays tagged as "mixed" for the data (points) and the likelihood function (histograms) in the Charge Dipole analysis.*

other than D mesons). In addition, a scale factor of 1.00 ± 0.05 (1.000 ± 0.025) is applied to the right-sign dipole tag probability for decays within $L < 0.5$ mm ($0.5 < L < 1.0$ mm) of the IP. This was done to take into account the somewhat higher mixed fraction seen in the data at small times (see Fig. 11). Dominant uncertainties are the B_s^0 production fraction in $Z^0 \to b\overline{b}$ events and the overall uncertainty in the final state tag purity, see Table 2.

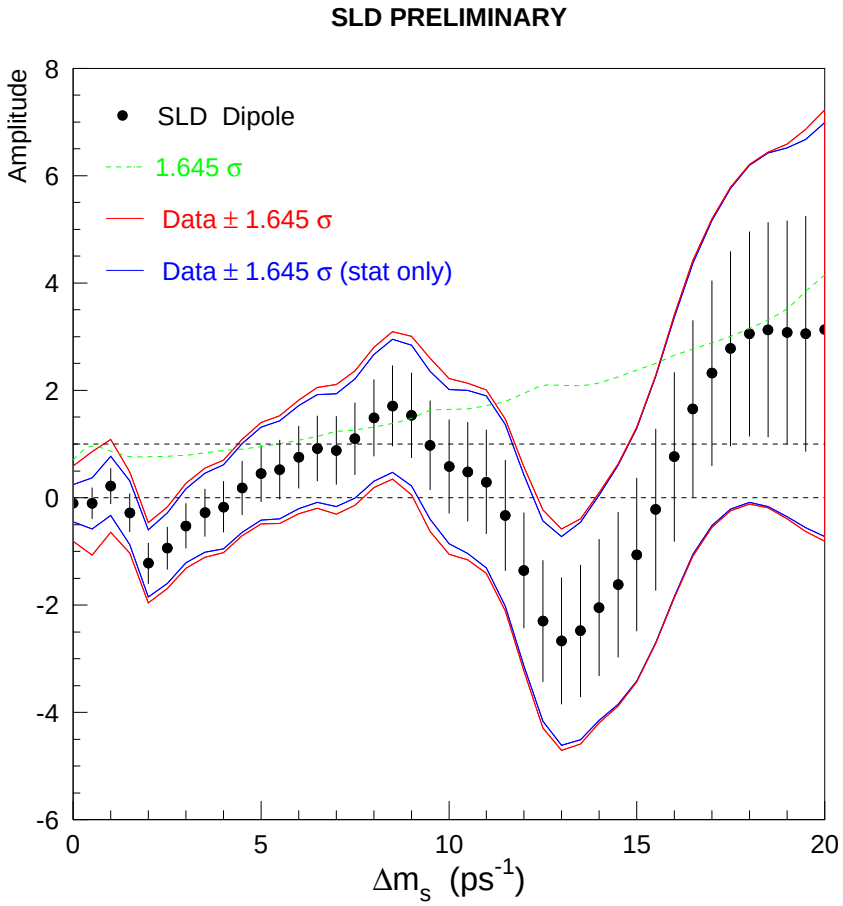

Figure 13: *Measured amplitude as a function of Δm_s in the Charge Dipole analysis.*

Table 2: Measured values of the oscillation amplitude A with a breakdown of systematic uncertainties for several Δm_s values in the Charge Dipole analysis.

Δm_s	5 ps^{-1}	10 ps^{-1}	15 ps^{-1}
Measured amplitude A	0.448	0.580	-1.060
σ_A^{stat}	± 0.527	± 0.874	± 1.431
σ_A^{syst}	$^{+0.242}_{-0.207}$	$^{+0.486}_{-0.464}$	$^{+0.198}_{-0.149}$
$f_s = \mathcal{B}(b \to B_s^0)$	$^{-0.149}_{+0.195}$	$^{-0.131}_{+0.165}$	$^{-0.095}_{+0.126}$
$f_\Lambda = \mathcal{B}(b \to b\text{−baryon})$	$^{+0.015}_{-0.021}$	$^{+0.011}_{-0.026}$	$^{+0.024}_{-0.023}$
$udsc$ fraction	$^{-0.007}_{+0.009}$	$^{-0.028}_{+0.024}$	$^{-0.010}_{+0.021}$
decay length resolution	$^{+0.019}_{-0.012}$	$^{+0.020}_{-0.017}$	$^{+0.059}_{-0.063}$
boost resolution	$^{+0.000}_{-0.010}$	$^{+0.289}_{-0.293}$	$^{-0.027}_{+0.081}$
b-hadron lifetimes	$^{+0.038}_{-0.033}$	$^{+0.014}_{-0.024}$	$^{+0.027}_{-0.027}$
Δm_d	$^{+0.001}_{-0.000}$	$^{+0.001}_{-0.004}$	$^{+0.003}_{-0.003}$
initial state tag	$^{+0.079}_{-0.087}$	$^{-0.015}_{+0.012}$	$^{-0.047}_{+0.048}$
final state tag	$^{+0.110}_{-0.107}$	$^{+0.352}_{-0.331}$	$^{+0.093}_{-0.072}$

6 Combination of the Analyses

The lepton+D, lepton+tracks and Charge Dipole analyses are combined taking into account correlated systematic errors. Events shared by two or more analyses are assigned to the analysis with the best sensitivity such as to produce statistically independent analyses. Figure 14 shows the measured amplitude as a function of Δm_s for the combination. As noted earlier, the measured values are consistent with $A = 0$ for the whole range of Δm_s up to 20 ps^{-1} and no evidence is found for a preferred value of the mixing frequency. The following ranges of B_s^0–$\overline{B_s^0}$ oscillation frequencies are excluded at 95% C.L.: $\Delta m_s < 5.2$ ps^{-1} and $11.3 < \Delta m_s < 14.2$ ps^{-1}, i.e., the condition $A + 1.645\,\sigma_A < 1$ is satisfied for those values. The combined sensitivity to set a 95% C.L. lower limit is found to be at a Δm_s value of 8.6 ps^{-1}. These results are preliminary.

It is worth noting that the overall sensitivity is expected to continue improving as the results of two more analysis techniques and further analysis refinements are implemented.

Acknowledgments

We thank the personnel of the SLAC accelerator department and the technical staffs of our collaborating institutions for their outstanding efforts.

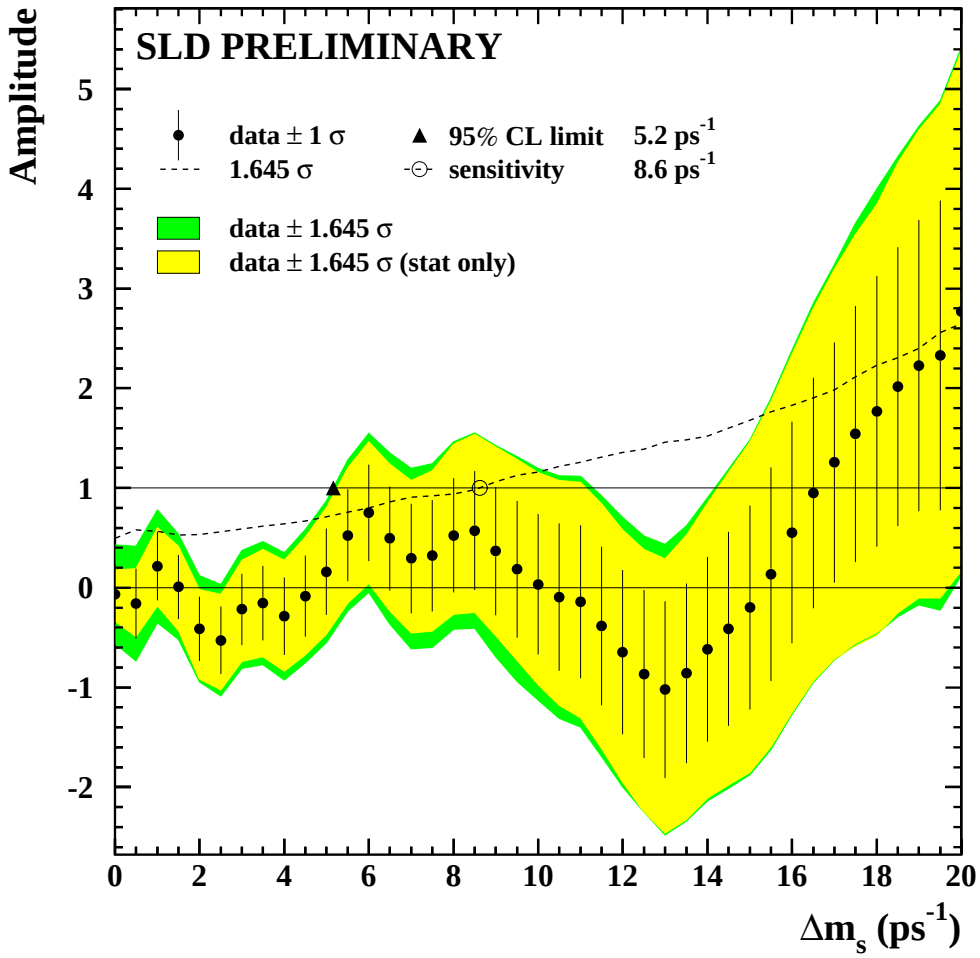

Figure 14: *Measured amplitude as a function of Δm_s for the lepton+D, lepton+tracks, and Charge Dipole analyses combined.*

References

[1] See the following reviews: P. Paganini, F. Parodi, P. Roudeau, and A. Stocchi, *Measurements of the ρ and η Parameters of the V_{CKM} Matrix and Perspectives*, Phys. Scripta **58**, 556 (1998), `hep-ph/9802289`, and `hep-ph/9903063`; S. Mele, Phys. Rev. **D59**, 113011 (1999).

[2] The lepton+tracks analysis was originally developed to study B^0_d–$\overline{B^0_d}$ mixing. The method is described in: K. Abe *et al.*, *Measurement of Time-Dependent $B^0_d - \overline{B^0_d}$ Mixing using Inclusive Semileptonic Decays*, SLAC-PUB-7228, July 1996.

[3] K. Abe *et al.*, Phys. Rev. **D53**, 1023 (1996).

[4] K. Abe *et al.*, Nucl. Inst. and Meth. **A400**, 287 (1997).

[5] T. Sjöstrand, Comp. Phys. Comm. **82**, 74 (1994).

[6] CLEO B decay model provided by P. Kim and the CLEO Collaboration.

[7] B. Barish *et al.*, Phys. Rev. Lett. **76**, 1570 (1996); H. Albrecht *et al.*, Z. Phys. **C58**, 191 (1993); H. Albrecht *et al.*, Z. Phys. **C62**, 371 (1994); P. Avery *et al.*, CLEO CONF 96-28, July 1996; L. Gibbons *et al.*, Phys. Rev. **D56**, 3783 (1997); T.E. Coan *et al.*, CLNS 97/1516; CLEO Collab., CLEO CONF 97-27, Aug. 1997; M. Zoeller, Ph.D. Thesis, SUNY Albany, 1994; X. Fu *et al.*, Phys. Rev. Lett. **79**, 3125 (1997); D. Gibaut *et al.*, Phys. Rev. **D53**, 4734 (1996).

[8] N. Isgur, D. Scora, B. Grinstein, and M.B. Wise, Phys. Rev. **D39**, 799 (1989).

[9] Particle Data Group, Phys. Rev. **D54**, Part I (1996).

[10] C. Peterson *et al.*, Phys. Rev. **D27**, 105 (1983).

[11] R. Brun *et al.*, Report No. CERN-DD/EE/84-1, 1989.

[12] D. J. Jackson, Nucl. Inst. and Meth. **A388**, 247 (1997).

[13] K. Abe *et al.* (SLD Collaboration), *Measurement of the B^+ and B^0 Lifetimes using Topological Vertexing at SLD*, SLAC-PUB-8206, July 1999, contributed paper # 477 to EPS-HEP99.

[14] K. Abe *et al.*, Phys. Rev. Lett. **80**, 660 (1998).

[15] K. Abe *et al.*, Phys. Rev. **D56**, 5310 (1997).

[16] H.-G. Moser and A. Roussarie, Nucl. Inst. and Meth. **A384**, 491 (1997).

[17] LEP B Oscillations Working Group, *Combined Results on B^0 Oscillations: Results from Winter 1999 Conferences*, LEPBOSC 99/1, June 1999.

** List of Authors

Kenji Abe,[21] Koya Abe,[33] T. Abe,[29] I. Adam,[29] T. Akagi,[29] H. Akimoto,[29] N.J. Allen,[5] W.W. Ash,[29] D. Aston,[29] K.G. Baird,[17] C. Baltay,[40] H.R. Band,[39] M.B. Barakat,[16] O. Bardon,[19] T.L. Barklow,[29] G.L. Bashindzhagyan,[20] J.M. Bauer,[18] G. Bellodi,[23] A.C. Benvenuti,[3] G.M. Bilei,[25] D. Bisello,[24] G. Blaylock,[17] J.R. Bogart,[29] G.R. Bower,[29] J.E. Brau,[22] M. Breidenbach,[29] W.M. Bugg,[32] D. Burke,[29] T.H. Burnett,[38] P.N. Burrows,[23] R.M. Byrne,[19] A. Calcaterra,[12] D. Calloway,[29] B. Camanzi,[11] M. Carpinelli,[26] R. Cassell,[29] R. Castaldi,[26] A. Castro,[24] M. Cavalli-Sforza,[35] A. Chou,[29] E. Church,[38] H.O. Cohn,[32] J.A. Coller,[6] M.R. Convery,[29] V. Cook,[38] R.F. Cowan,[19] D.G. Coyne,[35] G. Crawford,[29] C.J.S. Damerell,[27] M.N. Danielson,[8] M. Daoudi,[29] N. de Groot,[4] R. Dell'Orso,[25] P.J. Dervan,[5] R. de Sangro,[12] M. Dima,[10] D.N. Dong,[19] M. Doser,[29] R. Dubois,[29] B.I. Eisenstein,[13] I.Erofeeva,[20] V. Eschenburg,[18] E. Etzion,[39] S. Fahey,[8] D. Falciai,[12] C. Fan,[8] J.P. Fernandez,[35] M.J. Fero,[19] K. Flood,[17] R. Frey,[22] J. Gifford,[36] T. Gillman,[27] G. Gladding,[13] S. Gonzalez,[19] E.R. Goodman,[8] E.L. Hart,[32] J.L. Harton,[10] K. Hasuko,[33] S.J. Hedges,[6] S.S. Hertzbach,[17] M.D. Hildreth,[29] J. Huber,[22] M.E. Huffer,[29] E.W. Hughes,[29] X. Huynh,[29] H. Hwang,[22] M. Iwasaki,[22] D.J. Jackson,[27] P. Jacques,[28] J.A. Jaros,[29] Z.Y. Jiang,[29] A.S. Johnson,[29] J.R. Johnson,[39] R.A. Johnson,[7] T. Junk,[29] R. Kajikawa,[21] M. Kalelkar,[28] Y. Kamyshkov,[32] H.J. Kang,[28] I. Karliner,[13] H. Kawahara,[29] Y.D. Kim,[30] M.E. King,[29] R. King,[29] R.R. Kofler,[17] N.M. Krishna,[8] R.S. Kroeger,[18] M. Langston,[22] A. Lath,[19] D.W.G. Leith,[29] V. Lia,[19] C.Lin,[17] M.X. Liu,[40] X. Liu,[35] M. Loreti,[24] A. Lu,[34] H.L. Lynch,[29] J. Ma,[38] M. Mahjouri,[19] G. Mancinelli,[28] S. Manly,[40] G. Mantovani,[25] T.W. Markiewicz,[29] T. Maruyama,[29] H. Masuda,[29] E. Mazzucato,[11] A.K. McKemey,[5] B.T. Meadows,[7] G. Menegatti,[11] R. Messner,[29] P.M. Mockett,[38] K.C. Moffeit,[29] T.B. Moore,[40] M.Morii,[29] D. Muller,[29] V. Murzin,[20] T. Nagamine,[33] S. Narita,[33] U. Nauenberg,[8] H. Neal,[29] M. Nussbaum,[7] N. Oishi,[21] D. Onoprienko,[32] L.S. Osborne,[19] R.S. Panvini,[37] C.H. Park,[31] T.J. Pavel,[29] I. Peruzzi,[12] M. Piccolo,[12] L. Piemontese,[11] K.T. Pitts,[22] R.J. Plano,[28] R. Prepost,[39] C.Y. Prescott,[29] G.D. Punkar,[29] J. Quigley,[19] B.N. Ratcliff,[29] T.W. Reeves,[37] J. Reidy,[18] P.L. Reinertsen,[35] P.E. Rensing,[29] L.S. Rochester,[29] P.C. Rowson,[9] J.J. Russell,[29] O.H. Saxton,[29] T. Schalk,[35] R.H. Schindler,[29] B.A. Schumm,[35] J. Schwiening,[29] S. Sen,[40] V.V. Serbo,[29] M.H. Shaevitz,[9] J.T. Shank,[6] G. Shapiro,[15] D.J. Sherden,[29] K.D. Shmakov,[32] C. Simopoulos,[29] N.B. Sinev,[22] S.R. Smith,[29] M.B. Smy,[10] J.A. Snyder,[40] H. Staengle,[10] A. Stahl,[29] P. Stamer,[28] H. Steiner,[15] R. Steiner,[1] M.G. Strauss,[17] D. Su,[29] F. Suekane,[33] A. Sugiyama,[21] S. Suzuki,[21] M. Swartz,[14] A. Szumilo,[38] T. Takahashi,[29] F.E. Taylor,[19] J. Thom,[29] E. Torrence,[19] N.K. Toumbas,[29] T. Usher,[29] C. Vannini,[26] J. Va'vra,[29] E. Vella,[29] J.P. Venuti,[37] R. Verdier,[19] P.G. Verdini,[26] D.L. Wagner,[8] S.R. Wagner,[29] A.P. Waite,[29] S. Walston,[22] S.J. Watts,[5] A.W. Weidemann,[32] E. R. Weiss,[38] J.S. Whitaker,[6] S.L. White,[32] F.J. Wickens,[27] B. Williams,[8] D.C. Williams,[19] S.H. Williams,[29] S. Willocq,[17] R.J. Wilson,[10] W.J. Wisniewski,[29] J. L. Wittlin,[17] M. Woods,[29] G.B. Word,[37] T.R. Wright,[39] J. Wyss,[24] R.K. Yamamoto,[19] J.M. Yamartino,[19] X. Yang,[22] J. Yashima,[33] S.J. Yellin,[34] C.C. Young,[29] H. Yuta,[2] G. Zapalac,[39] R.W. Zdarko,[29] J. Zhou.[22]

(The SLD Collaboration)

[1] *Adelphi University, Garden City, New York 11530,*
[2] *Aomori University, Aomori , 030 Japan,*
[3] *INFN Sezione di Bologna, I-40126, Bologna, Italy,*
[4] *University of Bristol, Bristol, U.K.,*
[5] *Brunel University, Uxbridge, Middlesex, UB8 3PH United Kingdom,*
[6] *Boston University, Boston, Massachusetts 02215,*
[7] *University of Cincinnati, Cincinnati, Ohio 45221,*
[8] *University of Colorado, Boulder, Colorado 80309,*
[9] *Columbia University, New York, New York 10533,*
[10] *Colorado State University, Ft. Collins, Colorado 80523,*
[11] *INFN Sezione di Ferrara and Universita di Ferrara, I-44100 Ferrara, Italy,*
[12] *INFN Lab. Nazionali di Frascati, I-00044 Frascati, Italy,*
[13] *University of Illinois, Urbana, Illinois 61801,*
[14] *Johns Hopkins University, Baltimore, Maryland 21218-2686,*
[15] *Lawrence Berkeley Laboratory, University of California, Berkeley, California 94720,*
[16] *Louisiana Technical University, Ruston,Louisiana 71272,*
[17] *University of Massachusetts, Amherst, Massachusetts 01003,*
[18] *University of Mississippi, University, Mississippi 38677,*
[19] *Massachusetts Institute of Technology, Cambridge, Massachusetts 02139,*
[20] *Institute of Nuclear Physics, Moscow State University, 119899, Moscow Russia,*
[21] *Nagoya University, Chikusa-ku, Nagoya, 464 Japan,*
[22] *University of Oregon, Eugene, Oregon 97403,*
[23] *Oxford University, Oxford, OX1 3RH, United Kingdom,*
[24] *INFN Sezione di Padova and Universita di Padova I-35100, Padova, Italy,*
[25] *INFN Sezione di Perugia and Universita di Perugia, I-06100 Perugia, Italy,*
[26] *INFN Sezione di Pisa and Universita di Pisa, I-56010 Pisa, Italy,*
[27] *Rutherford Appleton Laboratory, Chilton, Didcot, Oxon OX11 0QX United Kingdom,*
[28] *Rutgers University, Piscataway, New Jersey 08855,*
[29] *Stanford Linear Accelerator Center, Stanford University, Stanford, California 94309,*
[30] *Sogang University, Seoul, Korea,*
[31] *Soongsil University, Seoul, Korea 156-743,*
[32] *University of Tennessee, Knoxville, Tennessee 37996,*
[33] *Tohoku University, Sendai 980, Japan,*
[34] *University of California at Santa Barbara, Santa Barbara, California 93106,*
[35] *University of California at Santa Cruz, Santa Cruz, California 95064,*
[36] *University of Victoria, Victoria, British Columbia, Canada V8W 3P6,*
[37] *Vanderbilt University, Nashville,Tennessee 37235,*
[38] *University of Washington, Seattle, Washington 98105,*
[39] *University of Wisconsin, Madison,Wisconsin 53706,*
[40] *Yale University, New Haven, Connecticut 06511.*